

## The use of interstation P wave arrival time differences to account for regional path variability

W. S. Phillips, C. A. Rowe, and L. K. Steck

Earth and Environmental Sciences Division, Los Alamos National Laboratory, Los Alamos, New Mexico, USA

Received 25 January 2005; revised 30 March 2005; accepted 4 May 2005; published 2 June 2005.

[1] The difference between arrival times from one seismic event to a pair of receivers is largely insensitive to source location error when certain geometric conditions are met. Using catalog data from a Chinese regional network, we illustrate the use of arrival time differences to control data quality and to derive a two-dimensional map of  $P_n$  velocity and relative site terms. The resulting velocity patterns follow regional geology closely, site terms reflect variations in crustal thickness, and both are consistent with previous work based on single ray methods. The model fits the time difference data to better than 1 s and we obtain a variance reduction of 75%. We believe that the continued development of time-difference techniques will lead to improved location accuracy and precision using regional network data. **Citation:** Phillips, W. S., C. A. Rowe, and L. K. Steck (2005), The use of interstation P wave arrival time differences to account for regional path variability, *Geophys. Res. Lett.*, 32, L11301, doi:10.1029/2005GL022558.

### 1. Introduction

[2] Travel times of regional seismic phases are strongly affected by heterogeneity in the crust and uppermost mantle. To improve location accuracy, we can account for heterogeneity by constructing three-dimensional models of seismic velocity [Firbas *et al.*, 1998; Johnson and Vincent, 2002; Murphy *et al.*, 2002; Ritzwoller *et al.*, 2003; Yang *et al.*, 2004; Pasyanos *et al.*, 2004], or regionally varying travel-time models [Bondar and North, 1999; Richards *et al.*, 2003]. We can also use empirical methods based on ground-truth (GT) information [Schultz *et al.*, 1998; Myers and Schultz, 2000], or, as many of these authors show, the two methods may be combined to take advantage of the strengths of both.

[3] Empirical methods are attractive because they account for velocity variation without requiring detailed knowledge of the structure. Unfortunately, high quality GT events (location known to 5 km or less) are rare. In many areas, we have an abundance of low quality GT events (20 km or greater) from teleseismic and regional catalogs. Location relative to the lower quality events will reflect any bias in the GT information; however, under certain conditions, these events can be used to obtain high quality arrival time difference data, which can, in turn, be used to obtain accurate path and site corrections.

[4] In the following, we explore the uses of regional arrival-time differences, and develop techniques that can be used to control data quality, as well as to obtain a two-dimensional path correction map and relative site terms, akin

to time-term  $P_n$  tomography methods. We will apply the techniques to data from the preliminary Annual Bulletin of Chinese Earthquakes (ABCE) [Lee *et al.*, 2002]. The success of the method will be judged by comparing results to known geological features, as well as to previous results based on standard methods. Quantitative studies of earthquake relocation will be reserved for the next stage of this study.

### 2. Method

[5] We obtain an earthquake location and consider the associated arrival times at two, regional distance stations. If the earthquake lies near the great circle passing through the two stations, but not between them, mislocation of the event has little effect on the arrival-time difference between stations. If the event falls between the two stations, however, mislocation has a large effect. We expect a gradation between these two end-member behaviors throughout the region surrounding the stations. We map this sensitivity for a grid of events by perturbing their locations, calculating transit times through a layered model and collecting statistics on the time differences. Results of one such calculation are plotted in Figure 1, showing extensive areas of stability beyond the expected regions along the interstation great circle. These stable regions are associated with  $P_n$  and upper mantle  $P$  propagation paths.

[6] Lateral variations in seismic velocity can be summarized by two-dimensional, station-centric correction surfaces [Schultz *et al.*, 1998] for use in location procedures. Every low sensitivity arrival-time difference becomes a precise constraint on the difference between two path correction surfaces in the epicentral area of that event. We began this effort by inverting for a full set of station-centric correction surfaces based on the time difference constraints. Too many degrees of freedom existed in that problem, however, and results of synthetic tests showed poor recovery of the true surfaces due to leakage of biased information into the model. We therefore adopted a tomographic formulation, which adds physical constraints to the problem that were not available for the correction surface inversion.

[7] Seismologists often use station differences to eliminate source effects from structural studies; examples include the determination of Rayleigh wave group velocity [e.g., Brilliant and Ewing, 1954], and the imaging of the upper mantle using teleseismic arrival times [e.g., Aki *et al.*, 1977]. Applying these ideas to a regional setting, for any low-sensitivity, event/two-station triple, we take the difference between two arrival-time residuals, based on preliminary locations, and write

$$\delta t_{ijk} = \sum_{l=1}^{N_{ik}} \delta x_{lik} \delta s_{lik} - \sum_{l=1}^{N_{jk}} \delta x_{ljk} \delta s_{ljk} + r_i - r_j \quad (1)$$

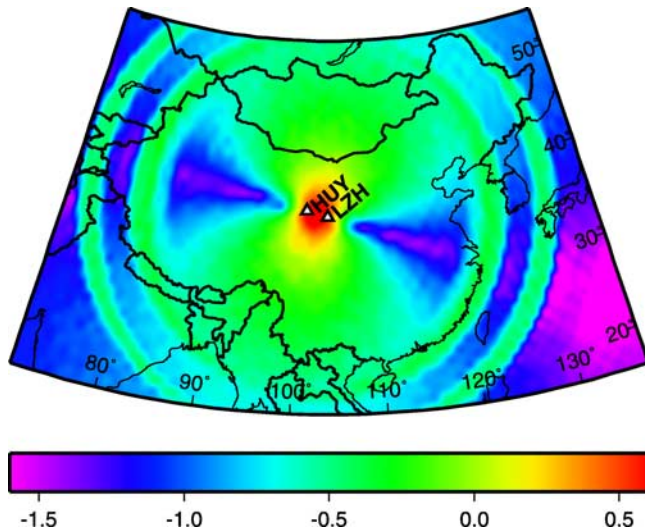


**Figure 1.** Sensitivity ( $\log_{10} s$ ) of arrival-time differences to changes in source location, calculated for stations HUY and LZH using the IASPEI earth model. At each grid point, sources were set at a depth of 20 km and perturbed in three dimensions using 200 realizations of 20 km Gaussian random noise. Perturbations above the surface were set to zero depth. Standard deviations of the time differences are plotted on a logarithmic scale. Rings at 1700 and 2300 km correspond to triplications produced by gradient changes in the uppermost mantle.

where  $i$  and  $j$  are station indices,  $k$  is the event index and  $l$  is a path summation index; the  $\delta s$  are slowness perturbations relative to the model used in location (IASPEI) [Kennett and Engdahl, 1991] and are interpolated from a grid of slownesses [e.g., Thurber, 1983] to the point at the center of each of  $N$  path segments. The  $\delta x$  are path segment lengths, constructed to be less than one-tenth of the slowness grid interval, and the  $r$  are site terms.

[8] We use the Vincenty [1975] method to obtain equally spaced points along great circle paths for a WGS84 ellipsoid for purposes of integrating through the slowness grid. Nonlinear effects of the velocity variations on ray geometry are ignored in our formulation, a common simplification for  $P_n$  work, which can lead to systematic bias in the velocity estimates for complex, three-dimensional structures [Hearn et al., 2004]. We then establish a linear system of equations based on Equation 1 and solve using conjugate gradient methods (LSQR) [Paige and Saunders, 1982] after applying first-difference constraints to adjacent grid parameters [e.g., Shaw and Orcutt, 1985; Phillips and Fehler, 1991]. The difference constraint weight ( $\lambda$ ) is chosen to maximize model variation while avoiding artifacts that would be introduced by noise. We damp the sum of the site terms to zero, to account for our lack of ability to determine their absolute level.

[9] Data from a well-distributed set of events for one pair of stations will constrain a linear combination of velocities, both between the stations, and for some distance normal to the interstation vector, and site terms. The tradeoff between velocities and site terms is resolved by combining data from many pairs of stations.

[10] We acknowledge that a velocity anomaly that is small in extent or in magnitude will produce a time

difference signal that can be smaller than our chosen, mislocation-induced sensitivity cutoff. To resolve small anomalies, we rely on the availability of sufficient data from the more insensitive geometries, and on the stacking effect from the remainder. Colinear geometries tightly constrain model parameters between stations, and the smoothing effect of the higher sensitivity difference data should be mitigated in areas of high station density. Conversely, we might expect less detail from time differences in areas of low station density, beyond the usual effects of lower ray path coverage. Clearly, further investigation of effects on image resolution of the sensitivity cutoff, or weighting based on sensitivity, would be worthwhile.

### 3. Data

[11] To study interstation time differences we used a preliminary version of the ABCE that has been made public [Lee et al., 2002], covering years from 1985 to 1999. We began by relocating the ABCE events using the IASPEI model. We then restricted data to distances between  $1.6^\circ$  and  $20^\circ$ , depths  $<50$  km, horizontal, 95% confidence location errors  $<100$  km, and arrival-time residuals  $<7.5$  s. This step limited phases to  $P_n$  and far-regional mantle  $P$  (although data from McNamara et al. [1997] show  $P_n$  velocities to 2000 km for paths through Tibet), and yielded nearly 1.5 million arrival-time differences. To ensure stability, we selected event/two-station triples for which 20 km random motion produced  $<1.6$  s scatter in the arrival-time differences ( $0.2 \log_{10} s$ , for comparison with Figure 1), and retained only that event yielding the median arrival-time difference in each half-degree grid cell for each station pair, requiring a minimum of 5 events per cell. This provided 20,415 high-quality arrival-time differences from 133 stations and 2819 events for use in the tomography. The latter step in the selection procedure reduced the number of arrival-time differences to  $<2\%$  of the earlier total, improving the data quality dramatically, and helping to avoid redundancy in the differenced data.

### 4. Results

[12] We performed the inversion by first requiring a smooth model ( $\lambda = 2000$ ), trimming data with residuals  $>3$  s, and re-inverting with a reduced constraint ( $\lambda = 1000$ ). This procedure eliminated a small number of outliers, most of which originated in weakly populated grid cells. The trimmed data inversions produced initial and final misfits (RMS) of 1.92 and 0.96 s, respectively, corresponding to a variance reduction of 75% (we assume data redundancy and the number of effective model parameters have little effect, thus RMS misfit can be used to obtain a reasonable estimate of residual variance).

[13] Lateral velocity variations and site terms are shown in Figures 2 and 3, respectively. Velocities reflect properties of the uppermost mantle and range from 7.7 to 8.3 km/s. Velocity is high across western China, particularly beneath the Sichuan, Tarim, Junggar, and Qaidam basins, all areas of competent media associated with relatively undeformed, accreted micro-continents. Velocity is low across eastern and southeast China and Indochina, suggesting higher mantle temperatures. We also see low velocities in Mongolia, north-central and eastern Tibet, the Qilian Shan and the

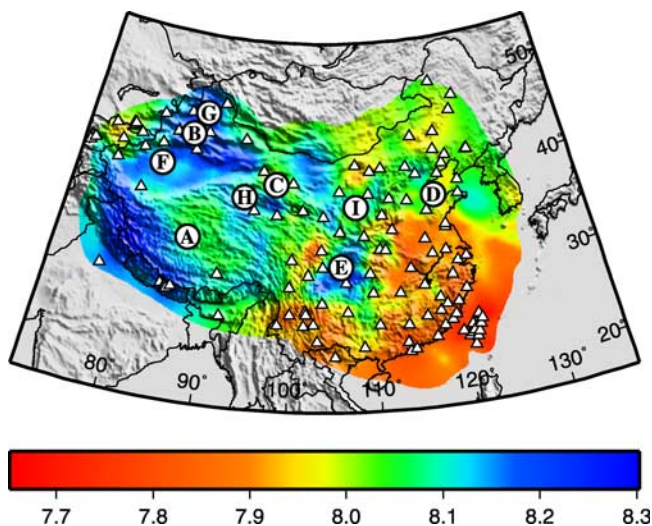


**Figure 2.** Velocity (km/s) of the mantle lid from the tomographic inversion of arrival-time residual differences. Velocity has been corrected for earth curvature based on a crustal thickness of 40 km. Triangles denote stations that provided data. The colored region is limited to standard errors  $<0.00035$  s/km and outlines the extent of the ray coverage for this data set. Regional features are labeled as follows: A) Tibet, B) Tian Shan, C) Qilian Shan, D) Bohai Sea, E) Sichuan Basin, F) Tarim Basin, G) Junggar Basin, H) Qaidam Basin, and I) Ordos Basin.

western Tian Shan. Site delays vary from  $-2$  to  $2$  s and reflect variations in crustal thickness and velocity. Delays are consistently low (early) across east and southeast China, and increase towards the Tibetan plateau and the Tian Shan. We also see some large delays for stations around the Bohai Sea that are not likely due to crustal thickness variations. Site delays for the same stations were found to be large for a “lower lid” (path lengths  $9^\circ$  to  $15^\circ$ ) inversion by *Hearn et al.* [2004], who note that upper mantle effects may be present in those results.

## 5. Discussion

[14] Our velocity image follows regional geology, and is qualitatively consistent with results from previous time-term  $P_n$  tomography studies [*McNamara et al.*, 1997; *Hearn et al.*, 2004; *Liang et al.*, 2004] and a three-dimensional model constructed from a composite of layered model inversions [*Sun et al.*, 2004]. These studies obtained similar mantle velocity ranges for this region, and the patterns outlined above match reasonably well, with some exceptions that may be related to differences in path coverage. Interestingly, the time-difference image shows velocities that are more stable across geological provinces, such as the Tarim and other basins. This may be due to effective culling of poor data using the gridded median described above, to the longer path-length limits and the possible influence of slightly deeper structure, to the use of first- rather than second-difference regularization, to the smoothing effect of the higher sensitivity time differences, or to the reduction of effects of event mislocation.

[15] *McNamara et al.* [1997], *Hearn et al.* [2004], *Liang et al.* [2004], and *Sun et al.* [2004] report RMS misfits ( $\sigma$ )

of 0.55, 1.3, 1.33 and 0.65 s, respectively. The misfit variations result from different quality control procedures in these studies. These misfit levels compare to that reported here (0.96 s) if we account for the increased error expected for a time difference  $((2\sigma^2)^{1/2} = 0.78, 1.8, 1.88$  and  $0.92$  s, respectively).

[16] The development of tomography models is one of many uses of interstation regional phase time differences. Stable time differences can also be used to evaluate independently constructed models (see references listed in the Introduction). Currently, only the best constrained events are used for such work. The use of time differences will greatly expand the number of events and the ensuing model coverage, however, assuming the models will not include near surface detail, will require relative site terms to be determined or introduced from independent studies.

[17] Time difference techniques can also be used to evaluate arrival-time picking error. By examining low-sensitivity arrival-time differences from northern California, *Rowe et al.* [2003] showed that data error increased dramatically for paths along fault zones, ascribing this to a combination of poor propagation conditions and nodal take-off angles. An expected stable time difference that is anomalous relative to neighboring events indicates that one or both arrival times are poorly determined. A simple inversion that compares all stable pairs will assign error estimates to individual arrival times. These error estimates can be used to cull data sets, and may even be useful for data weighting or correction; however, the latter idea will require detailed investigation before confidence can be assured.

[18] *Pavlis and Booker* [1980] and *Spencer and Gubbins* [1980] discuss techniques that decouple location and velocity model portions of a joint inversion, thus desensitizing velocity results to some level of mislocation, as does the method described here. These parameter separation techniques may be applied to the  $P_n$  time-term problem by solving for epicentral location and a source term that combines origin time and depth, which cannot be resolved independently, and performing the decoupling as the method directs, using the null space of the resulting three-column

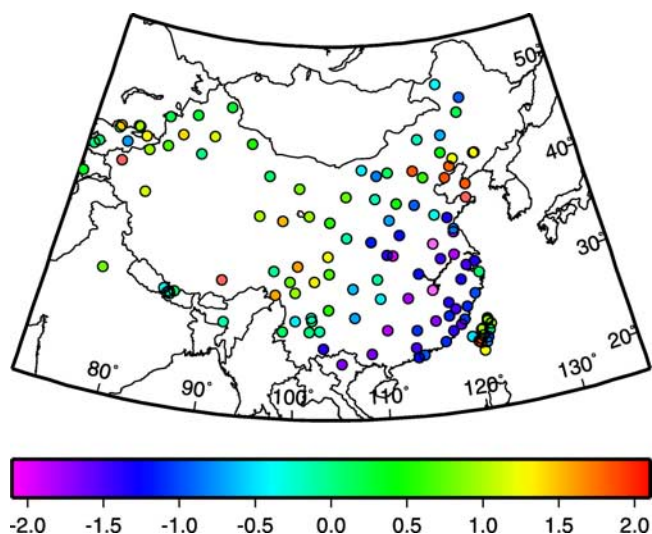


**Figure 3.** Relative site delay (s) from the tomographic inversion of arrival-time residual differences.

location matrix. This is an attractive alternative to the tomography portion of the method described here. Irrespective of the tomography method used, we believe that the data quality control provided by the time difference analysis will remain critical to this type of study.

## 6. Conclusions

[19] We have discussed the identification of interstation arrival-time differences that are stable with respect to event mislocation, their use in data quality control, and the development of a tomographic technique used to obtain laterally varying velocity and site terms for China and surrounding regions. Results follow regional geology and crustal thickness and show qualitative agreement with the results of some previous  $P_n$  inversion studies in the region that were based on single path inversion methods. The velocities we obtain are smoother within individual geological provinces, while matching the range of variation of previous studies, likely a consequence of the quality control afforded by the time differences, but perhaps also from the longer paths, decreased effects of mislocation, smoothing effects of high sensitivity differences, or style of regularization. Testing the model's ability to improve location accuracy with sparse sub-networks is the next step in verifying this method.

[20] Interstation time difference techniques can also be used to evaluate travel-time models, normally performed using a small number of rare, high quality GT events, thus allowing much greater coverage and validation of a model. Time differences can also be used to estimate arrival-time errors through consistency between neighboring events, which will further contribute to quality control efforts.

[21] **Acknowledgments.** We gratefully acknowledge discussions with Bill Rodi and Tom Hearn that have helped to guide our study. In addition, Richard Stead placed catalog information into CSS database tables and performed background quality control. Two anonymous reviewers supplied constructive comments that helped to improve the manuscript, and that will impact our future development of these ideas. We used GMT software for Figures 1–3. This research was supported by the US DOE under Contract W-7405-ENG-36, LA-UR-05-0649.

## References

- Aki, K., A. Christofferson, and E. S. Husebye (1977), Determination of the three-dimensional seismic structure of the lithosphere, *J. Geophys. Res.*, **82**, 277–296.
- Bondar, I., and R. G. North (1999), Development of calibration techniques for the Comprehensive Nuclear Test-Ban Treaty (CTBT) international monitoring system, *Phys. Earth Planet. Inter.*, **113**, 11–24.
- Brilliant, R. M., and M. Ewing (1954), Dispersion of Rayleigh waves across the U.S., *Bull. Seismol. Soc. Am.*, **44**, 149–158.
- Firbas, P., K. Fuchs, and W. D. Mooney (1998), Calibration of seismograph network may meet test ban treaty's monitoring needs, *Eos Trans. AGU*, **79**, 413.
- Hearn, T. M., S. Wang, J. F. Ni, Z. Xu, Y. Yu, and X. Zhang (2004), Uppermost mantle velocities beneath China and surrounding regions, *J. Geophys. Res.*, **109**, B11301, doi:10.1029/2003JB002874.
- Johnson, M., and C. Vincent (2002), Development and testing of a 3D velocity model for improved event location; a case study for the India-Pakistan region, *Bull. Seismol. Soc. Am.*, **92**, 2893–2910.
- Kennett, B. L. N., and E. R. Engdahl (1991), Traveltimes for global earthquake location and phase identification, *Geophys. J. Int.*, **105**, 429–465.
- Lee, W. H. K., H. Kanamori, P. C. Jennings, and C. Kisslinger (Eds.) (2002), *International Handbook of Earthquake and Engineering Seismology* [CD-ROM], Elsevier, New York.
- Liang, C., X. Song, and J. Huang (2004), Tomographic inversion of Pn traveltimes in China, *J. Geophys. Res.*, **109**, B11304, doi:10.1029/2003JB002789.
- McNamara, D. E., W. R. Walter, T. J. Owens, and C. J. Ammon (1997), Upper mantle velocity structure beneath the Tibetan Plateau from Pn travel time tomography, *J. Geophys. Res.*, **102**, 493–505.
- Murphy, J., et al. (2002), Seismic calibration of Group 1 International Monitoring System (IMS) stations in eastern Asia for improved event location, paper presented at 24th Seismic Research Review, Sept. 17–19, Natl. Nucl. Security Admin., Ponte Vedra, Fla.
- Myers, S. C., and C. A. Schultz (2000), Improving sparse network seismic location with Bayesian kriging and teleseismically constrained calibration events, *Bull. Seismol. Soc. Am.*, **90**, 199–211.
- Paige, C. C., and M. A. Saunders (1982), Algorithm 583, LSQR: Sparse linear equations and least-squares problems, *Trans. Math. Software*, **8**, 195–209.
- Pasyanos, M. E., W. R. Walter, M. P. Flanagan, P. Goldstein, and J. Bhattacharyya (2004), Building and testing an a priori geophysical model for western Eurasia and North Africa, *Pure Appl. Geophys.*, **161**, 235–281.
- Pavlis, G. L., and J. R. Booker (1980), The mixed discrete-continuous inverse problem: Application to the simultaneous determination of earthquake hypocenters and velocity structure, *J. Geophys. Res.*, **85**, 4801–4810.
- Phillips, W. S., and M. C. Fehler (1991), Traveltime tomography: A comparison of popular methods, *Geophysics*, **56**, 1639–1649.
- Richards, P., et al. (2003), Seismic location calibration for 30 International Monitoring System stations in Eastern Asia: Final results, paper presented at 25th Seismic Research Review, Sept. 23–25, Natl. Nucl. Security Admin., Tucson, Ariz.
- Ritzwoller, M. H., N. M. Shapiro, A. Levshin, E. A. Bergman, and R. R. Engdahl (2003), The ability of a global 3-D model to locate regional events, *J. Geophys. Res.*, **108**(B7), 2353, doi:10.1029/2002JB002167.
- Rowe, C. A., W. S. Phillips, and L. K. Steck (2003), Relative constraints on correction surfaces for more effective use of low-order ground truth, *Eos Trans. AGU*, **84**(46), Fall Meet. Suppl., Abstract S21D-0332.
- Schultz, C. A., S. C. Myers, J. Hipp, and C. J. Young (1998), Nonstationary Bayesian kriging: A predictive technique to generate spatial corrections for seismic detection, location and identification, *Bull. Seismol. Soc. Am.*, **88**, 1275–1288.
- Shaw, P. R., and J. A. Orcutt (1985), Waveform inversion of seismic refraction data and applications to young Pacific crust, *Geophys. J. R. Astron. Soc.*, **82**, 375–414.
- Spencer, C., and D. Gubbins (1980), Travel time inversion for simultaneous earthquake location and velocity structure determination in laterally varying media, *Geophys. J. R. Astron. Soc.*, **63**, 95–116.
- Sun, Y., X. Li, S. Kuleli, F. D. Morgan, and M. N. Toksoz (2004), Adaptive moving window method for 3D P-velocity tomography and its application in China, *Bull. Seismol. Soc. Am.*, **94**, 740–746.
- Thurber, C. H. (1983), Earthquake locations and three-dimensional crustal structure in the Coyote Lake area, central California, *J. Geophys. Res.*, **88**, 8226–8236.
- Vincenty, T. (1975), Direct and inverse solutions of geodesics on the ellipsoid with application of nested equations, *Surv. Rev.*, **23**, 88–93.
- Yang, X., I. Bondar, J. Bhattacharyya, M. Ritzwoller, N. Shapiro, M. Antolik, G. Ekstrom, H. Israelsson, and K. McLaughlin (2004), Validation of regional and teleseismic travel-time models by relocating ground-truth events, *Bull. Seismol. Soc. Am.*, **94**, 897–919.

W. S. Phillips, C. A. Rowe, and L. K. Steck, Earth and Environmental Sciences Division, MS D408, Los Alamos National Laboratory, Los Alamos, NM 87545, USA. (wsp@lanl.gov; char@lanl.gov; lsteck@lanl.gov)